Journal of Power Sources 188 (2009) 57–63

Contents lists available at ScienceDirect

Journal of Power Sources

journal homepage: www.elsevier.com/locate/jpowsour

Synthesis and properties of sulfonated poly(arylene ether phosphine oxide)s for proton exchange membranes

Xuhui Ma, Chunjie Zhang, Guyu Xiao*, Deyue Yan*

College of Chemistry and Chemical Engineering, the State Key Laboratory of Metal Matrix Composites, Shanghai Jiao Tong University, 800 Dongchuan Road, Shanghai 200240, P.R. China

ARTICLE INFO

Article history:
Received 7 October 2008
Received in revised form
16 November 2008
Accepted 17 November 2008
Available online 28 November 2008

Keywords:
Poly(arylene ether phosphine oxide)s
Proton exchange membrane
Sulfonate

ABSTRACT

A series of sulfonated poly(arylene ether phosphine oxide)s (sPAEPO) were prepared by direct polycondensation of sulfonated bis(4-fluorophenyl)phenyl phosphine oxide and bis(4-fluorophenyl)phenyl phosphine oxide with various diphenol-type monomers. The resulting ionomers show high molecular weight and excellent thermal stability. The bisphenol moieties of sPAEPO greatly affect the properties. sPAEPO-NA, -Bis A, -BP, and -6F show excellent dimensional stability. However, sPAEPO-DB and -HQ indicate abrupt swelling even at 80 and 90 °C, respectively, unsuitable for proton exchange membranes. In contrast, sPAEPO-6F with the lowest swelling exhibits the highest conductivity of 7.68×10^{-2} S cm^{-1} among all the sPAEPO, close to that of Nafion 117. Besides, sPAEPO-NA and -Bis A show a worse oxidative stability than other sPAEPO (sPAEPO-Bis A, -BP, -HQ, and -6F) due to the naphthalene ring and the isopropylidene unit in the backbone, respectively. Contrary to sPAEPO-Bis A and -BP, sPAEPO-NA and -6F exhibit well connective ionic domains owing to the high hydrophobic nature of the naphthalene ring and hexafluoroisopropylidene moieties. The connected ionic domains provide sPAEPO-NA and -6F with higher proton conductivity in comparison with sPAEPO-Bis A and -BP. In conclusion, sPAEPO-6F has the best comprehensive properties among all the sPAEPO, indicating a promising prospect in proton exchange membrane applications.

1. Introduction

Proton exchange membrane fuel cells (PEMFC) have attracted more and more attention as green power sources due to the low emission, low noise, and high efficiency. Proton exchange membrane (PEM) is one of key components of PEMFC, which serves as the conducting medium of the proton, the separator of the reactant gas, and the carrier of the catalyst [1]. Nafion is the state-of-the-art membrane used as PEM for its overall properties. However, Nafion suffers from some technical limitations such as a remarkable loss of proton conductivity at low humidity or high temperature, high methanol crossover, and expensive cost [2,3]. Therefore, this urges the necessity to explore alternative non-fluorinated proton exchange membranes for fuel cell applications [3].

Great efforts have been made to develop non-fluorinated proton exchange membranes [1,3–7]. A series of high performance polymers were utilized as the matrix to prepare the corresponding PEM one after the other, including sulfonated poly(arylene ether ketone)s [8,9], sulfonated poly(arylene ether sulfone)s [10,11], sulfonated poly(arylene thioether)s [12,13], sulfonated poly(*p*-phenylene)s [14], sulfonated polyimides [15–18], sulfonated polyphosphazenes [19], sulfonated poly(phthalazinone ether)s [20–23], sulfonated polybenzimidazoles [24–27], sulfonated polyoxadiazoles [28], sulfonated polybenzoxazoles [29,30] and so on.

As a kind of high performance polymer, poly(arylene ether phosphine oxide)s possess high mechanical properties, high thermal stability, and chemical stability [31]. Moreover, the phosphine oxide group is favorable to enhance the water retention of materials and adhesive ability with inorganic compounds [32]. Therefore, they show great interest as the matrix of PEM. Up to now, there are few reports on PEM derived from poly(arylene ether phosphine oxide)s. McGrath and co-workers [33] firstly reported sulfonated poly(arylene ether phosphine oxide)s (sPAEPO) in a conference proceeding, the properties related to PEM are very limited. Subsequently, our group prepared sulfonated poly(phthalazinone ether phosphine oxide)s and sulfonated poly(arylene thioether phosphine oxide)s, which showed excellent properties [34,35]. This paper synthesized a series of sulfonated poly(arylene ether phosphine oxide)s by polycondensation of sulfonated bis(4-fluorophenyl)phenyl phosphine oxide (sBFPPO) and bis(4-fluorophenyl)phenyl phosphine oxide (BFPPO) with various diphenol-type monomers, respectively, including bisphenol A (Bis A), 4,4'-dihydroxybiphenyl (DB), hydroquinone (HQ), 4,4'-biphenol (BP), 1,5-dihydroxynaphthalene (NA), and 4,4'-

* Corresponding authors. Fax: +86 21 54741297.
E-mail addresses: gyxiao@sjtu.edu.cn (G. Xiao), dyyan@sjtu.edu.cn (D. Yan).

0378-7753/$ – see front matter © 2008 Elsevier B.V. All rights reserved.
doi:10.1016/j.jpowsour.2008.11.090

(hexafluoroisopropylidene)diphenol (6F). They are characterized in detail so as to evaluate whether they are suitable for PEM applications or not.

2. Experimental

2.1. Materials

Phenylphosphonic dichloride was purchased from Aldrich and used as received. Bis A, DB, HQ, BP, NA, and 6F were purchased from commercial sources and purified by recrystallization and dried *in vacuo* before use. *N*-Methyl-2-pyrrolidone (NMP) was dehydrated by azeotropic distillation with benzene and distilled under reduced pressure and stored over 4 Å molecular sieves. Toluene was distilled before use. Anhydrous potassium carbonate was dried at 150 °C for 24 h under reduced pressure prior to use. 4-Bromofluorobenzene, magnesium, fuming sulfonic acid, and other chemicals were obtained commercially and used without further purification. BFPPO and sBFPPO were prepared according to our previous report [34,35].

2.2. Synthesis of polymers

A series of sulfonated poly(arylene ether phosphine oxide)s were synthesized by direct polycondensation of sBFPPO and BFPPO with the diphenol-type monomers like Bis A, DB, HQ, BP, NA, and 6F, respectively. sPAEPO-xx represents sPAEPO derived from various bisphenol monomers, for example, sPAEPO-Bis A was prepared from Bis A. Although the reactivity of the bisphenols was somewhat different, the polymerization procedure was similar. The synthesis of sPAEPO-HQ was selected as a typical example. To a three-necked round flask equipped with a mechanical stirrer, a Dean–Stark trap with a condenser, and a nitrogen gas inlet/outlet were charged 0.4404 g (0.004 mol) of HQ, 0.9992 g (0.0024 mol) of sBFPPO, 0.5028 g (0.0016 mol) of BFPPO, 0.6081 g (0.0044 mol) of K_2CO_3, 8 ml NMP, and 8 ml toluene. The reaction mixture was stirred at refluxing temperature for 4 h to dehydrate by azeotropic distillation with toluene, then the temperature was increased to 175 °C and toluene was removed from the reaction mixture by a nitrogen flow. The temperature was kept at 175 °C for 4 h, 190 °C for 12 h, and 200 °C for 48 h to obtain a very viscous solution. After being cooled to 110 °C, the viscous solution was diluted with 2 ml of NMP and poured into 300 ml of de-ionized water with vigorous stirring, producing the fibrous polymer. The inorganic salt within the resultants was removed by soaking them in hot water for several days. The product was dried under vacuum at 100 °C for 48 h.

Yield: 97%. FT-IR (film, cm^{-1}): 1175 ($Ar_3P{=}O$), 1105, 1033, 617 ($Ar{-}SO_3Na$). ^1H NMR (DMSO-d_6, ppm): 7.95–7.88 (0.6 H), 7.85–7.78 (0.6 H), 7.64–7.45 (7.2 H), 7.25–7.15 (4 H), 7.15–7.05 (4 H).

2.3. Preparation of membranes

sPAEPO in the salt form were dissolved in dimethyl sulfoxide (DMSO). The polymers solution were cast onto a dust-free glass plate and dried at 65 °C for 3 days. Thereafter, the glass plate was immersed in de-ionized water for several minutes, the transparent, tough, and flexible membranes peeled off from the glass plate. The membranes in the acid form were obtained by soaking them in a 1 M HCl for 24 h, followed by submersing in de-ionized water for another 24 h. The thickness of the membranes was about 40 μm.

2.4. Instruments

NMR spectra were recorded on a Varian MERCURY plus 400 MHz spectrometer using deuterated dimethyl sulfoxide (DMSO-d_6) as solvent and tetramethylsilane as internal standard sample. FT-IR spectra were performed on a Bruker Equinox-55 Fourier transform spectrometer and the polymers thin films were utilized as testing samples. The molecular weight of products was determined by a PE Series 200 gel permeation chromatography (GPC) equipped a refractive index detector. All samples were run in *N*,*N*-dimethylformamide (DMF) containing 0.05 M LiBr at room temperature with a flow rate of 1.0 ml min^{-1}. Polystyrene standards were used for calibration. The thermal stability was conducted on a PE TGA-7 thermogravimetric analyzer (TGA). The acid form samples for TGA analysis were heated at 150 °C for 30 min under a nitrogen flow to remove moisture and then cooled to 90 °C. The measurement was carried out from 90 to 800 °C at a heating rate of 20 °C min^{-1}. The glass transition temperature (T_g) of the polymers were determined on a PE Pyris-1 differential scanning calorimeter (DSC). The samples in the acid form for DSC analysis were preheated under nitrogen protection at 150 °C for 30 min to dehydrate and then cooled to 80 °C. The DSC curves were recorded from 80 to 400 °C at a heating rate of 10 °C min^{-1}. Atomic force microscopy (AFM) measurement was carried out on a Digital Instrument (DI) NanoScopeIII under tapping mode.

2.5. Ion exchange capacity

The ion exchange capacity (IEC) of sulfonated polymers was determined by titration. Before testing, the acid form membranes were soaked in the saturated NaCl solution for 48 h so as to librate the H^+ to the solution by ion exchange with the Na^+. Then the released H^+ was titrated with the NaOH solution using phenolphthalein as an indicator. The value of IEC was obtained by the following equation:

$$\mathrm{IEC} = \frac{N_{\mathrm{NaOH}} \times V_{\mathrm{NaOH}}}{W_{\mathrm{dry}}} \times 100\%$$

where N_{NaOH}, V_{NaOH}, and W_{dry} were the concentration, the consumed volume of NaOH solution, and the weight of the dry membrane, respectively.

2.6. Water uptake and swelling

The water uptake and swelling were determined by measuring the change of weight and size between the wet and dry membrane. The acid form membrane was dried at 120 °C under vacuum for 24 h until the weight is constant. The weight and size of the dry membrane were recorded as a benchmark. The dry membrane was immersed in de-ionized water at the given temperatures for the same interval (24 h) and then taken out and wiped off water on the surface quickly. After the weight and size of the wet membrane were measured, the water uptake and swelling could be obtained by the following equations:

$$\text{water uptake} = \frac{W_{\mathrm{wet}} - W_{\mathrm{dry}}}{W_{\mathrm{dry}}} \times 100\%$$

$$\text{swelling} = \frac{(L_{\mathrm{wet}} - L_{\mathrm{dry}}}{L_{\mathrm{dry}}} \times 100\%$$

where W_{wet} and W_{dry} were the mass of the wet and dry membrane, L_{wet} and L_{dry} were the length of the wet and dry membrane, respectively.

2.7. Oxidative stability

The oxidative stability of the resulting membranes in the acid form was examined by Fenton's test (3% H_2O_2 containing 2 ppm $FeSO_4$) at 70 °C. The size of the samples is 15 mm × 15 mm and the thickness is about 6 μm. The oxidative stability of the membranes was determined by the dissolving behavior in Fenton's reagent.

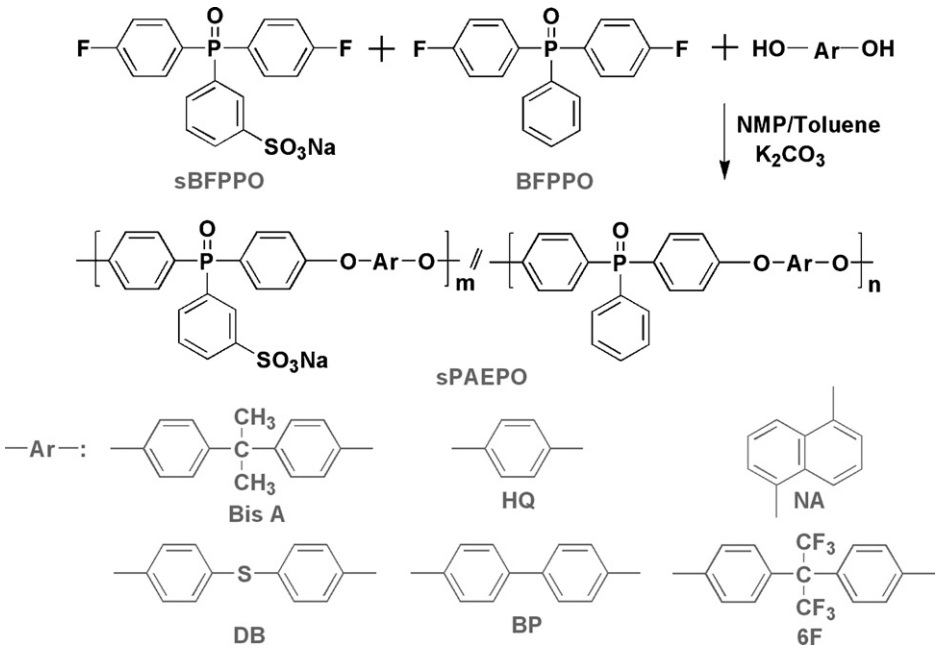

Scheme 1. Preparation of sPAEPO.

2.8. Proton conductivity

The proton conductivity of membranes was evaluated by a solatron 1260 gain phase analyzer over a frequency range from 10^7 to 1 Hz like a previous procedure [34]. The samples (20 mm × 8 mm) were clamped between two electrodes and rinsed several times with ultrapure water, then soaked in ultrapure water for 48 h. The measurement of proton conductivity was carried out after the membrane was soaked in ultrapure water for 0.5 h at a given temperature. The proton conductivity (σ) of samples in the longitudinal direction was calculated by the formula $\sigma = L/(RA)$, where L and A are the distance between two electrodes and cross-sectional area of the membrane, respectively. R is the resistance of the membrane.

3. Results and discussion

3.1. Synthesis and characterization of polymers

Sulfonated poly(arylene ether phosphine oxide)s were prepared via the aromatic nucleophilic substitution polycondensation of sBFPPO and BFPPO with the diphenol-type monomers (Bis A, DB, HQ, BP, NA, and 6F) in a NMP/toluene solvent system, respectively, using K_2CO_3 as weak base (Scheme 1). The diphenol-type monomers in the reaction mixture were converted into the corresponding bisphenol anions by K_2CO_3, which attacked the activated carbon atoms (connected with F) of sBFPPO and BFPPO to produce the resulting polymers. The results of polycondensation are tabulated in Table 1. sPAEPO-Bis A, -DB, -NA, and -6F show the molecular weight higher than 2.6×10^4 g mol^{-1} and the polydispersity index (PDI) of 1.66–3.32. However, the molecular weight of sPAEPO-HQ and -BP could not be obtained by gel permeation chromatogram due to the poor solubility in DMF. But both of them could be cast into transparent, tough, and flexible membranes, indicating that they have high molecular weight. The structure of bisphenol monomers greatly affected the polymerization reaction. For example, the highest reaction temperature and longest reaction time were needed for sPAEPO-6F to obtain high molecular weight among all the sPAEPO. This is due to the low nucleophilicity of the 6F anions, resulting from the strong electron-withdrawing hexafluoroisopropylidene group at the *para*-position of the phenolic OH group. In contrast, sPAEPO-Bis A with a high molecular weight can be obtained under the mild polymerization conditions, which is attributed to the high nucleophilicity and flexible isopropylidene group of the bisphenol A anions.

Table 1
The results of polycondensation.

Ionomers	sBFPPO/BFPPO (molar ratio)	GPC			Yield (%)
		$M_n \times 10^{-4}$	$M_w \times 10^{-4}$	PDI	
sPAEP0-Bis A	80/20	4.44	8.21	1.85	97
sPAEPO-DB	80/20	3.85	9.09	2.36	96
sPAEPO-HQ	60/40	–[a]	–[a]	–[a]	97
sPAEPO-BP	70/30	–[a]	–[a]	–[a]	98
sPAEPO-NA	70/30	2.62	4.34	1.66	97
sPAEPO-6F	90/10	2.90	9.63	3.32	96

[a] Poor solubility in DMF.

FT-IR spectra of all the sPAEPO are displayed in Fig. 1. The absorption band at 1175 cm^{-1} is assigned to the stretching vibration of phosphine oxide groups. All the samples exhibit the characteristic peaks at 1105 and 1032 cm^{-1}, which are attributed to the asymmetric and symmetric stretching vibration of the sulfone group of $-SO_3Na$, respectively. The absorption band centred at 617 cm^{-1} is ascribed to the S–O of the sulfonate group. These indicate that the

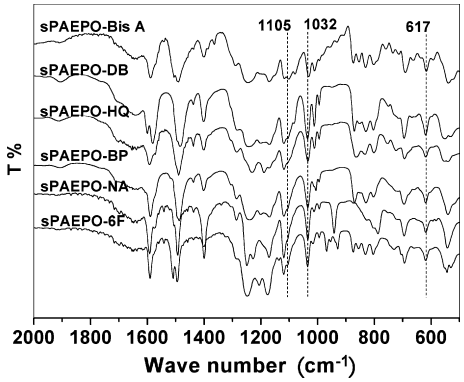

Fig. 1. FT-IR spectra of sPAEPO.

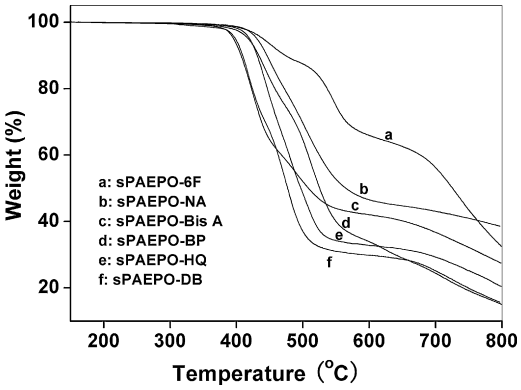

Fig. 2. TGA curves of sPAEPO.

Table 2
The properties of sPAEPO.

Ionomers	T_g (°C)	T_{d5} (°C)	IEC (meq. g^{-1})	
			The calculated	The measured
sPAEPO-Bis A	257	395	1.41	1.32
sPAEPO-DB	330	398	1.44	1.31
sPAEPO-HQ	353	418	1.39	1.38
sPAEPO-BP	354	420	1.36	1.28
sPAEPO-NA	360	430	1.43	1.33
sPAEPO-6F	380	440	1.32	1.24

sulfonate groups were successfully attached onto the backbone of the products.

3.2. Thermal properties of sulfonated polymers

The TGA curves of sPAEPO are displayed in Fig. 2. For sPAEPO-Bis A, -DB, -BP, and -6F, the TGA curves show a distinct two-step degradation pattern, whereas those of sPAEPO-HQ and -NA almost look like a one-step degradation profile though they are really a two-step degradation pattern if they are observed carefully. The first weight loss temperature is at about 380 °C, which is assigned to desulfonation, and the second weight loss step is in the range of 450–510 °C, due to the polymer main chain degradation. This is similar to the previous reports [9]. The 5% mass loss temperature (T_{d5}) of the ionomers is summarized in Table 2. As seen from Table 2, the T_{d5} of the sulfonated polymers is higher than 390 °C, showing high thermal stability. Moreover, the bisphenol moieties of sPAEPO affect the thermal stability. For example, sPAEPO-DB indicates the T_{d5} of 398 °C, while sPAEPO-6F with an equal ion exchange capacity shows the T_{d5} of 440 °C.

The glass transition of the sulfonated polymers in the acid form is determined by DSC. No endothermic peak and exothermic peak are found in the DSC curves. The glass transition temperature (T_g) of them is listed in Table 2. As can be seen from Table 2, the bisphenol structure has a great effect on the T_g. sPAEPO-Bis A and -DB, with the flexible groups in the backbones, show a low T_g, while other sPAEPO denote a T_g higher than 350 °C. It is worthwhile mentioning that sPAEPO-Bis A and -6F exhibit the lowest T_g of 257 °C and the highest T_g of 380 °C among all the sPAEPO, respectively. Comparing the chemical structure of sPAEPO-Bis A with that of sPAEPO-6F, the difference between them is that the flexible groups (except the ether bonds) of the former in the backbone are the isopropylidene moieties whereas those of the latter are the hexafluoroisopropylidene moieties, so it can be concluded that the lowest T_g of sPAEPO-Bis A is attributed to the high flexible group of the isopropylidene unit while the highest T_g of sPAEPO-6F is related to the increased stiffness arising from the hexafluoroisopropylidene unit. The similar phenomenon was also found in the studies of Guiver and co-workers [36].

3.3. Ion exchange capacity

The IEC of the sulfonated polymers are evaluated by titration and summarized in Table 2. The IEC values of sPAEPO, determined by the feed ratios, are adjusted to a narrow range of 1.32–1.44 meq. g^{-1} so as to evaluate the effect of diphenol moieties on the properties of resulting products. It can be seen from Table 2 that all the experimental values of IEC coincide well with the calculated one, suggesting that all of the sulfonated monomers were incorporated into the backbone by direct polycondensation without side reactions, which were often observed in the post-sulfonation procedure.

3.4. Water uptake and swelling

It is well known that many properties of proton exchange membranes are closely related to their water content. In the vehicle mechanism, the water within the membrane is necessary for PEM to conduct protons since it is the carrier of the proton conduction. However, excessive water content may lead to the undesirable large swelling and a dramatic loss of the mechanical strength. Therefore, the absorbed water in PEM is very important for PEM [5]. Compared with the post-sulfonation method, the direct polycondensation has the advantage of adjusting the IEC of resultants by changing the feed ratios of the sulfonated monomer to the un-sulfonated monomer. Because both the bisphenol moiety and the IEC of sPAEPO affect the water content of PEM, the IEC of various sPAEPO was adjusted to the comparable range of 1.32–1.44 meq. g^{-1} in order to investigate the effect of bisphenol moieties on the water uptake and swelling of the

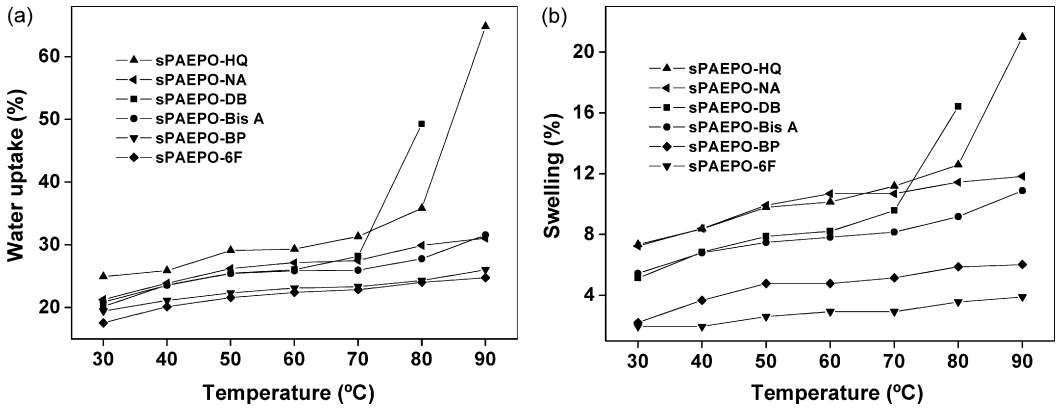

Fig. 3. (a) Water uptake and (b) swelling of sPAEPO membranes at various temperatures.

Table 3
The oxidative stability of sPAEPO membranes.

Ionomers	sPAEPO-Bis A	sPAEPO-DB	sPAEPO-HQ	sPAEPO-BP	sPAEPO-NA	sPAEPO-6F
τ_1 (min)	30	45	40	50	23	47
τ_2 (min)	420	443	441	510	261	470

τ_1: the time when the membrane started to break into pieces.
τ_2: the time when the membrane dissolved completely.

resulting membranes. The water uptake and swelling of membrane samples with various bisphenol units as a function of temperatures are plotted in Fig. 3(a and b), respectively. It can be seen from Fig. 3(a) that the water uptake of all the membranes increases with increasing temperatures. At the same time, the bisphenol units of sPAEPO also have a great effect on water uptake. For sPAEPO-NA, -Bis A, -BP, and -6F, the water uptake enhances slowly at the entire temperature range studied. The water uptake of them at 80 °C are 29.9%, 27.8%, 24.3%, and 24.0%, respectively, slightly less than that (30%) of Nafion 117. sPAEPO-6F exhibits the lowest water uptake among them because of the hydrophobic nature of the hexafluoroisopropylidene units in the backbone, similar to the previous report [36]. On the other hand, the water uptake of sPAEPO-DB and -HQ shows an abrupt increase at 80 and 90 °C, respectively.

As can be seen from Fig. 3(b), the profile of swelling curves of sPAEPO is very like that of water uptake curves. In the case of sulfonated poly(arylene ether)s, this phenomenon is also found [11]. sPAEPO-NA, -Bis A, -BP, and -6F show a slow increasing swelling with the increase of temperatures. The swelling of them at 80 °C are only 11.5%, 9.2%, 5.9%, and 3.6%, respectively, much lower than that (20%) of Nafion 117. This demonstrates that they exhibit excellent dimensional stability. Similar to the profile of water uptake curves, the swelling curves of sPAEPO-DB and -HQ denote a suddenly enhancement at 80 and 90 °C, respectively. In general, this kind of membranes loses most of the mechanical strength due to excessive swelling, unsuitable for PEM applications [5].

3.5. Oxidative stability

The perfluorinated proton exchange membranes possess excellent oxidative stability. Up to now, the oxidative stability of the hydrocarbon PEM is still a key issue for fuel cell applications [7,37]. Generally, the oxidative stability is evaluated by comparing the time when membrane samples started to break into pieces (τ_1) and dissolved completely (τ_2) in Fenton's reagent (3% H_2O_2 containing 2 ppm $FeSO_4$). The value of τ_1 and τ_2 is shown in Table 3. As can be seen from Table 3, sPAEPO-NA and -Bis A show a worse stability to oxidation than other sPAEPO. sPAEPO-NA contains the naphthalene units, which exhibit lower aromatic properties than the benzene units. On the other hand, sPAEPO-Bis A has aliphatic connecting units (isopropylidene groups) in the backbone, easily attacked by peroxide free radicals. Consequently, the naphthalene and isopropylidene units provide sPAEPO-NA and -Bis A with a low resistance to oxidation, respectively. In addition, sPAEPO-HQ, -DB, -BP, and -6F did not dissolve in Fenton's reagent for 440 min, indicating that they show a comparable oxidative stability to other aromatic PEM [7,38].

To our interest, the previous sulfonated poly(arylene thioether phosphine oxide)s (sPATPO), with an equal sulfonation degree, shows much better oxidative stability than sPAEPO-DB. The reason is briefly explained in the Supplementary materials [39]. The investigation relevant to the oxidative stability of sPATPO would be further carried out in our future work.

3.6. Proton conductivity

PEM combines the hydrophobic backbone with the hydrophilic pendant groups, as lead to the hydrophilic/hydrophobic nanophase separation morphology. The hydrophobic backbone provides the mechanical strength while the hydrated hydrophilic domain is responsible for the proton conduction [5]. The water within the PEM is the carrier of the proton conduction, but excessive water content make PEM lose the mechanical strength or even dissolvable [5]. As mentioned above, sPAEPO-DB and -HQ is not suitable for PEM due to excessive swelling at elevated temperatures, so the measurement of proton conductivity was carried out only for sPAEPO-NA, -Bis A, -BP, and -6F. The proton conductivity of the membranes as a function of temperatures is shown in Fig. 4. As expected, the proton conductivity of all the samples increases with increasing temperatures. It is worthwhile noting that the proton conductivity of sPAEPO-NA, -Bis A, and -BP increases in turn at a given temperature. This increasing sequence of proton conductivity is exactly that of the water uptake at a given temperature, which is shown in Fig. 3(a). This is attributed to the fact that the conductivity of PEM enhances with increasing water uptake in a definite range of water content. The similar phenomenon was reported in the literature [35]. The proton conductivities of them at 80 °C are 2.32×10^{-2}, 3.53×10^{-2}, and 4.88×10^{-2} S cm^{-1}, respectively. In contrast, in the case of sPAEPO-6F, the water uptake is lowest, but the proton conductivity is highest among all the sPAEPO in the entire temperature range studied. The proton conductivity of sPAEPO-6F at 80 °C is 7.68×10^{-2} S cm^{-1}, which is close to that of Nafion 117. Probably, the reason arises from the microscopic structure of sPAEPO-6F. In general, the hydrocarbon based PEM with high proton conductivity suffer from excessive swelling. However, the membrane from sPAEPO-6F shows high proton conductivity as well as dimensional stability, which is attractive for fuel cell applications.

3.7. Microstructure of membranes

The microstructure of membranes heavily affects their macroscopic properties such as the water uptake, swelling, and proton conductivity [11,35,38]. The tapping mode AFM phase images of sPAEPO under ambient conditions were recorded on a 500 nm × 500 nm size scale. Similar to the study of proton conductivity, the investigation of microscopic morphology was performed only for sPAEPO-NA, -Bis A, -BP, and -6F since sPAEPO-HQ and -DB show excessive swelling and are unsuitable for fuel cell applications. The AFM phase images are shown in Fig. 5. As can be

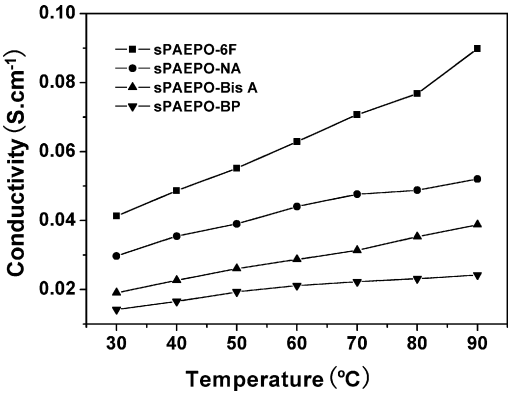

Fig. 4. Proton conductivity of sPAEPO membranes at various temperatures.

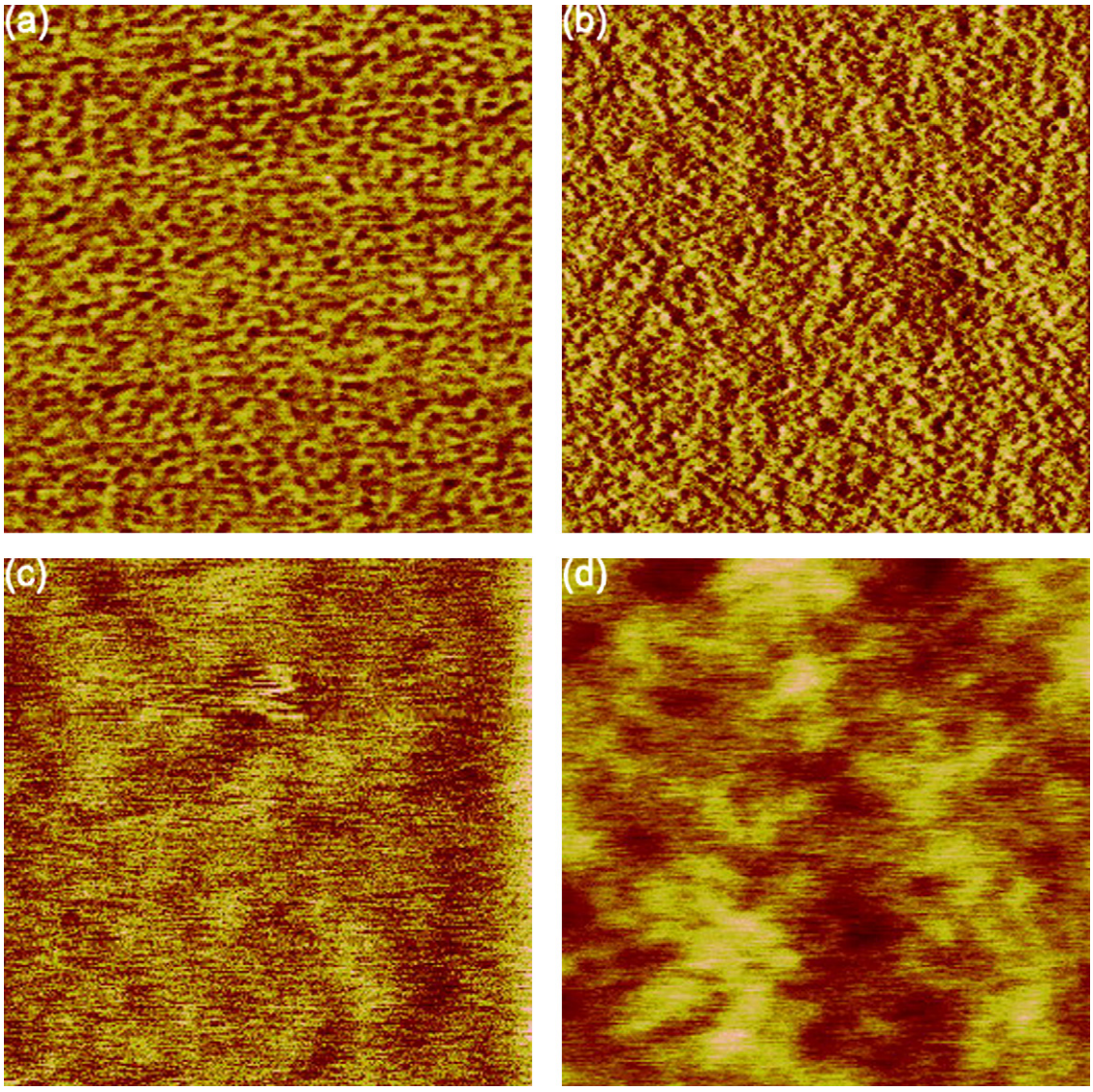

Fig. 5. The AFM phase images of: (a) sPAEPO-Bis A, (b) sPAEPO-BP, (c) sPAEPO-NA, (d) sPAEPO-6F.

seen from Fig. 5, all samples show nanophase separated morphology as indicated by the dark and bright regions. The dark regions are attributed to the hydrophilic sulfonic acid groups, responsible for proton conduction, whereas the bright regions are related to the hydrophobic units, endowing the membrane with mechanical strength [5,11]. The AFM phase images of sPAEPO-Bis A and -BP exhibit many segregated ionic domains in the continuous hydrophobic matrix, the proton conducts difficultly through the hydrated ionic domains. On the contrary, sPAEPO-NA shows well connective ionic domains. In the case of sPAEPO-6F, the nanophase separation becomes more obvious in comparison with sPAEPO-NA. These are probably due to the higher hydrophobic nature of the naphthalene ring and hexafluoroisopropylidene moieties compared with other diphenol moieties and favorable to form the connective ion channel, resulting in high conductivity like the previous report [36].

4. Conclusions

A series of sulfonated poly(arylene ether phosphine oxide)s were synthesized via polycondensation of sulfonated bis(4-fluorophenyl)phenyl phosphine oxide and bis(4-fluorophenyl)phenyl phosphine oxide with various diphenol-type monomers. The resulting sulfonated polymers exhibit excellent thermal stability. The bisphenol moieties of sPAEPO have a great effect on the water uptake, swelling, oxidative stability, proton conductivity, and microstructure. For sPAEPO-NA, -Bis A, -BP, and -6F, the water uptakes and swelling at 80 °C are less than 30% and 12%, respectively. However, sPAEPO-DB and -HQ show excessive swelling even at 80 and 90 °C, respectively, unsuitable for fuel cell applications. In contrast, sPAEPO-6F with the lowest swelling showed the highest conductivity of 7.68×10^{-2} S cm^{-1} among all the sPAEPO, close to that of Nafion 117. sPAEPO-NA and -Bis A show a worse oxidative stability than other sPAEPO due to the naphthalene ring and the isopropylidene unit in the backbone, respectively. It is noteworthy that sulfonated poly(arylene thioether phosphine oxide)s (sPATPO-80) indicate much better resistance to oxidation than sPAEPO-DB with a similar chemical structure. The AFM phase images illustrated that sPAEPO-Bis A and -BP exhibit many dispersive ionic domains and that sPAEPO-NA and -6F possess well connected ionic domains owing to the high hydrophobic nature of the naphthalene ring and hexafluoroisopropylidene moieties. The connected ionic domains endow sPAEPO-NA and -6F with higher proton conductivity compared with sPAEPO-Bis A and -BP. In conclusion, sPAEPO-6F has the

best comprehensive properties among all the sPAEPO, suggesting that it is a promising PEM material.

Acknowledgements

This research was supported by the National Natural Science Foundation of China (no: 50303010 and 50633010), the National High Technical Research Development Program (no: 2002AA323040), the Shanghai Leading Academic Discipline Project (no: B202), and the Science and Technology Committee of Shanghai municipality (no: 065207065).

Appendix A. Supplementary data

Supplementary data associated with this article can be found, in the online version, at doi:10.1016/j.jpowsour.2008.11.090.

References

[1] J. Rozière, D.J. Jones, Annu. Rev. Mater. Res. 33 (2003) 503–555.
[2] M. Rikukawa, K. Sanui, Prog. Polym. Sci. 25 (2000) 1463–1502.
[3] M.A. Hickner, H. Ghassemi, Y.S. Kim, B.R. Einsla, J.E. McGrath, Chem. Rev. 104 (2004) 4587–4612.
[4] J.A. Kerres, J. Membr. Sci. 185 (2001) 3–27.
[5] K.D. Kreuer, J. Membr. Sci. 185 (2001) 29–39.
[6] O. Savadogo, J. Power Sources 127 (2004) 135–161.
[7] Q.F. Li, R.H. He, J.O. Jensen, N.J. Bjerrum, Chem. Mater. 15 (2003) 4896–4915.
[8] G.Y. Xiao, G.M. Sun, D.Y. Yan, Polym. Bull. 48 (2002) 309–315.
[9] S. Zhong, T. Fu, Z. Dou, C. Zhao, H. Na, J. Power Sources 162 (2006) 51–57.
[10] M. Ueda, H. Toyota, T. Ouchi, J. Sugiyama, K. Yonetake, T. Masuko, T. Teramoto, J. Polym. Sci. Part A: Polym. Chem. 31 (1993) 853–858.
[11] J. Pang, H. Zhang, X. Li, Z. Jiang, Macromolecules 40 (2007) 9435–9442.
[12] G.Y. Xiao, G.M. Sun, D.Y. Yan, Polym. Prep. 44 (2003) 1235–1236.
[13] B. Zongwu, M.F. Durstock, T.D. Dang, J. Membr. Sci. 281 (2006) 508–516.
[14] T. Kobayashi, M. Rikukawa, K. Sanui, N. Ogata, Solid State Ionics 106 (1998) 219–225.
[15] S. Faure, N. Cornet, O. Geibel, R. Mercier, M. Pineri, B. Sillion, New Materials for Fuel Cell and Modern Battery Systems II, Ecole Polytech, Montreal, 1997, pp. 818–827.
[16] H. Zhou, K. Miyatake, M. Watanabe, Fuel Cells 5 (2005) 296–301.
[17] X.X. Guo, J.H. Fang, K. Tanaka, H. Kita, K. Okamoto, J. Polym. Sci. Part A: Polym. Chem. 42 (2004) 1432–1440.
[18] N. Li, Z. Cui, S. Zhang, S. Li, F. Zhang, J. Power Sources 172 (2007) 511–519.
[19] H.R. Allcock, M.A. Hofmann, C.M. Ambler, R.V. Morford, Macromolecules 35 (2002) 3484–3489.
[20] G.Y. Xiao, G.M. Sun, D.Y. Yan, Macromol. Rapid Commun. 23 (2002) 488–492.
[21] G.Y. Xiao, G.M. Sun, D.Y. Yan, P.F. Zhu, P. Tao, Polymer 43 (2002) 5335–5339.
[22] H.W. Zhang, C.H. Du, Y.Y. Xu, B.K. Zhu, Polym. Adv. Technol. 18 (2007) 373–378.
[23] Y.L. Chen, Y.Z. Meng, A.S. Hay, Macromolecules 38 (2005) 3564–3566.
[24] M.B. Gieselman, J.R. Reynolds, Macromolecules 25 (1992) 4832–4834.
[25] M. Kawahara, M. Rikukawa, K. Sanui, N. Ogata, Solid State Ionics 136–137 (2000) 1193–1196.
[26] J.A. Asensio, S. Borrós, P. Gómez-Romero, J. Polym. Sci. Part A: Polym. Chem. 40 (2002) 3703–3710.
[27] S.B. Qing, W. Huang, D.Y. Yan, J. Polym. Sci. Part A: Polym. Chem. 43 (2005) 4363–4372.
[28] D. Gomes, J. Roeder, M.L. Ponce, S.P. Nunes, J. Power Sources 175 (2008) 49–59.
[29] B.R. Einsla, Y.J. Kim, C. Tchatchoua, J.E. Mcgrath, Polym. Prep. 44 (2003) 645–646.
[30] N. Tan, G.Y. Xiao, D.Y. Yan, Polym. Bull., submitted for publication.
[31] S. Wang, H. Zhuang, H.K. Shobha, T.E. Glass, M. Sankarapandian, Q. Ji, A.R. Shultz, J.E. McGrath, Macromolecules 34 (2001) 8051–8063.
[32] D.J. Riley, A. Gungor, S.A. Srinivason, M. Sankarapandian, C.N. Tchatchoua, M.W. Muggli, T.C. Ward, J.E. McGrath, Polym. Eng. Sci. 37 (1997) 1501–1511.
[33] H.K. Shobha, G.R. Smalley, M. Sankarapandian, J.E. McGrath, Polym. Prep. 41 (2000) 180–181.
[34] X.H. Ma, L.P. Shen, C.J. Zhang, G.Y. Xiao, D.Y. Yan, G.M. Sun, J. Membr. Sci. 310 (2008) 303–311.
[35] X.H. Ma, C.J. Zhang, G.Y. Xiao, D.Y. Yan, G.M. Sun, J. Polym. Sci. Part A: Polym. Chem. 46 (2008) 1758–1769.
[36] P.X. Xing, G.P. Robertson, M.D. Guiver, S.D. Mikhailenko, S. Kaliaguine, Macromolecules 37 (2004) 7960–7967.
[37] J.L. Zhang, Z. Xie, J.J. Zhang, Y.H. Tang, C.J. Song, T. Navessin, Z.Q. Shi, D. Song, H.J. Wang, D.P. Wilkinson, Z.S. Liu, S. Holdcroft, J. Power Sources 160 (2006) 872–891.
[38] B.J. Liu, G.P. Robertson, D.S. Kim, M.D. Guiver, W. Hu, Z.H. Jiang, Macromolecules 40 (2007) 1934–1944.
[39] See the supplementary materials.